7 Transmission Lines Redux

7 Transmission Lines Redux

7.1 Parallel Wire Transmission Line

A parallel wire transmission line consists of wires separated by a dielectric spacer. Figure 7.1 shows a common implementation, commonly known as “twin lead.” The wires in twin lead line are held in place by a mechanical spacer comprised of the same low-loss dielectric material that forms the jacket of each wire. Very little of the total energy associated with the electric and magnetic fields lies inside this material, so the jacket and spacer can usually be neglected for the purposes of analysis and electrical design.

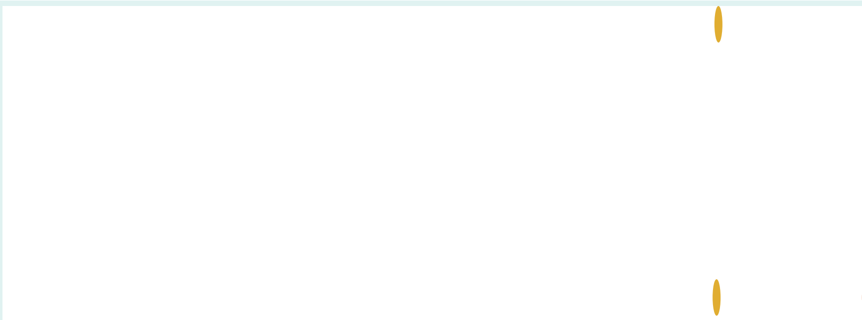

Figure 7.1. *Twin lead, a commonly-encountered form of parallel wire transmission line.*

© *SpinningSpark, Inductiveload CC BY SA 3.0 (https://creativecommons.org/licenses/by-sa/3.0/) (modified)*

Parallel wire transmission line is often employed in radio applications up to about 100 MHz as an alternative to coaxial line. Parallel wire line has the advantages of lower cost and lower loss than coaxial line in this frequency range. However, parallel wire line lacks the self-shielding property of coaxial cable; i.e., the electromagnetic fields of coaxial line are isolated by the outer conductor, whereas those of parallel wire line are exposed and prone to interaction with nearby structures and devices. This prevents the use of parallel wire line in many applications.

Another discriminator between parallel wire line and coaxial line is that parallel wire line is differential.[1] The conductor geometry is symmetric and neither conductor is favored as a signal datum (“ground”). Thus, parallel wire line is commonly used in applications where the signal sources and/or loads are also differential; common examples are the dipole antenna and differential amplifiers.[2]

Figure 7.2 shows a cross-section of parallel wire line.

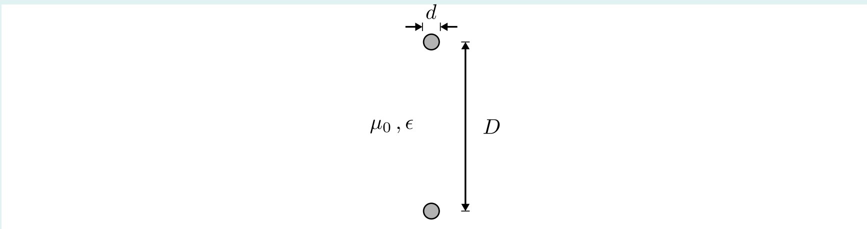

Figure 7.2. *Parallel wire transmission line structure and design parameters.*

Relevant parameters include the wire diameter, d; and the center-to-center spacing, D.

The associated field structure is transverse electromagnetic (TEM) and is therefore completely described by a single cross-section along the line, as shown in Figure 7.3.

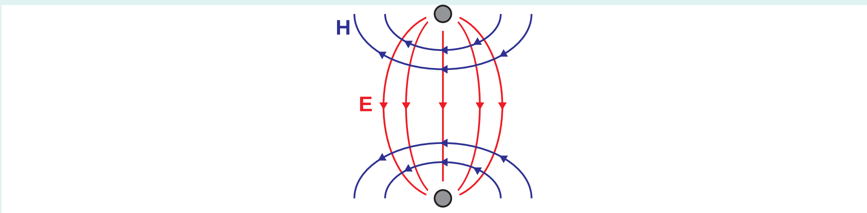

Figure 7.3. *Structure of the electric and magnetic fields for a cross-section of parallel wire line. In this case, the wave is propagating away from the viewer.*

Expressions for these fields exist, but are complex and not particularly useful except as a means to calculate other parameters of interest. One of these parameters is, of course, the characteristic impedance since this parameter plays an important role in the analysis and design of systems employing transmission lines. The characteristic impedance may be determined using the "lumped element" transmission line model using the following expression:

$$Z_0 = \sqrt{\frac{R' + j\omega L'}{G' + j\omega C'}} \tag{7.1}$$

where R', G', C', and L' are the resistance, conductance, capacitance, and inductance per unit length, respectively. This analysis is considerably simplified by neglecting loss; therefore, let us assume the "low-loss" conditions $R' \ll \omega L'$ and $G' \ll \omega C'$. Then we find:

$$Z_0 \approx \sqrt{\frac{L'}{C'}} \quad \text{(low loss)} \tag{7.2}$$

and the problem is reduced to determining inductance and capacitance of the transmission line. These are

$$L' = \frac{\mu_0}{\pi} \ln\left[(D/d) + \sqrt{(D/d)^2 - 1}\right] \tag{7.3}$$

$$C' = \frac{\pi\epsilon}{\ln\left[(D/d) + \sqrt{(D/d)^2 - 1}\right]} \tag{7.4}$$

Because the wire separation D is typically much greater than the wire diameter d, $D/d \gg 1$ and so $\sqrt{(D/d)^2 - 1} \approx D/d$. This leads to the simplified expressions

$$L' \approx \frac{\mu_0}{\pi} \ln\left(2D/d\right) \quad (D \gg d) \tag{7.5}$$

$$C' \approx \frac{\pi\epsilon}{\ln\left(2D/d\right)} \quad (D \gg d) \tag{7.6}$$

Now returning to Equation 7.2:

$$Z_0 \approx \frac{1}{\pi}\sqrt{\frac{\mu_0}{\epsilon}} \ln\left(2D/d\right) \tag{7.7}$$

Noting that $\epsilon = \epsilon_r \epsilon_0$ and $\sqrt{\mu_0/\epsilon_0} \triangleq \eta_0$, we obtain

$$\boxed{Z_0 \approx \frac{1}{\pi} \frac{\eta_0}{\sqrt{\epsilon_r}} \ln\left(2D/d\right)} \tag{7.8}$$

The characteristic impedance of parallel wire line, assuming low-loss conditions and wire spacing much greater than wire diameter, is given by Equation 7.8.

Observe that the characteristic impedance of parallel wire line increases with increasing D/d. Since this ratio is large, the characteristic impedance of parallel wire line tends to be large relative to common values of other kinds of TEM transmission line, such as coaxial line and microstrip line. An example follows.

Example

Example 7.1

$300~\Omega$ twin-lead.

A commonly-encountered form of parallel wire transmission line is $300~\Omega$ twin-lead. Although implementations vary, the wire diameter is usually about 1 mm and and the wire spacing is usually about 6 mm. The relative permittivity of the medium $\epsilon_r \approx 1$ for the purposes of calculating transmission line parameters, since the jacket and spacer have only a small effect on the fields. For these values, Equation 7.8 gives $Z_0 \approx 298~\Omega$, as expected.

Under the assumption that the wire jacket/spacer material has a negligible effect on the electromagnetic fields, and that the line is suspended in air so that $\epsilon_r \approx 1$, the phase velocity v_p for a parallel wire line is approximately that of any electromagnetic wave in free space; i.e., c. In practical twin-lead, the effect of a plastic jacket/spacer material is to reduce the phase velocity by a few percent up to about 20%, depending on the materials and details of construction. So in practice $v_p \approx 0.8c$ to $0.9c$ for twin-lead line.

Additional Reading:

- "Twin-lead (https://en.wikipedia.org/wiki/Twin-lead)" on Wikipedia.
- "Differential signaling (https://en.wikipedia.org/wiki/Differential_signaling)" on Wikipedia.
- Sec. 8.7 ("Differential Circuits") in S.W. Ellingson, *Radio Systems Engineering*, Cambridge Univ. Press, 2016.

---

1. The references in "Additional Reading" at the end of this section may be helpful if you are not familiar with this concept. ↩
2. This is in contrast to "single-ended" line such as coaxial line, which has conductors of different cross-sections and the outer conductor is favored as the datum. ↩

7.2 Microstrip Line Redux

A microstrip transmission line consists of a narrow metallic trace separated from a metallic ground plane by a slab of dielectric material, as shown in Figure 7.4. This is a natural way to implement a transmission line on a printed circuit board, and so accounts for an important and expansive range of applications. The reader should be aware that microstrip is distinct from *stripline*, which is a distinct type of transmission line; see "Additional Reading" at the end of this section for disambiguation of these terms.

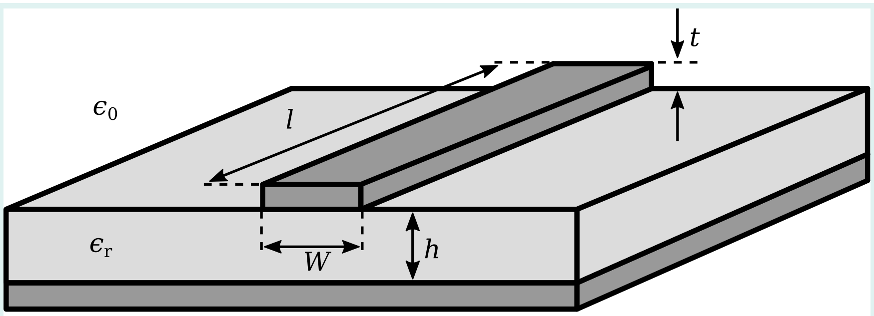

Figure 7.4. *Microstrip transmission line structure and design parameters.*

A microstrip line is single-ended[1] in the sense that the conductor geometry is asymmetric and the one conductor – namely, the ground plane – also normally serves as ground for the source and load.

The spacer material is typically a low-loss dielectric material having permeability approximately equal to that of free space ($\mu \approx \mu_0$) and relative permittivity ϵ_r in the range of 2 to about 10 or so.

The structure of a microstrip line is similar to that of a parallel plate waveguide (Section 6.6), with the obvious difference that one of the "plates" has finite length in the direction perpendicular to the direction of propagation. Despite this difference, the parallel plate waveguide provides some useful insight into the operation of the microstrip line. Microstrip line is nearly always operated below the cutoff frequency of all but the TM$_0$ mode, whose cutoff frequency is zero. This guarantees that only the TM$_0$ mode can propagate. The TM$_0$ mode has the form of a uniform plane wave, as shown in Figure 7.5. The electric field is oriented in the direction perpendicular to the plates, and magnetic field is oriented in the direction parallel to the plates. The direction of propagation $\mathbf{E} \times \mathbf{H}$ for the TM$_0$ mode always points in the same direction; namely, along the axis of the transmission line. Therefore, microstrip lines nominally exhibit transverse electromagnetic (TEM) field structure.

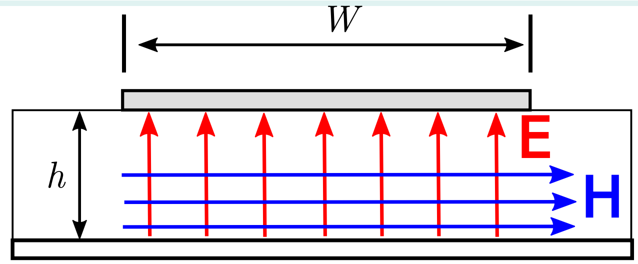

Figure 7.5. *Approximate structure of the electric and magnetic fields within microstrip line, assuming TM$_0$ operation. The fields outside the line are possibly significant, complicated, and not shown. In this case, the wave is propagating away from the viewer.*

The limited width W of the trace results in a "fringing field" – i.e., significant deviations from TM$_0$ field structure in the dielectric beyond the edges of the trace and above the trace. The fringing fields may play a significant role in determining the characteristic impedance Z_0. Since Z_0 is an important parameter in the analysis and design of systems using transmission lines, we are motivated to not only determine Z_0 for the microstrip line, but also to understand how variation in W affects Z_0. Let us address this issue by considering the following three special cases, in order:

- $W \gg h$, which we shall refer to as the "wide" case.
- $W \ll h$, which we shall refer to as the "narrow" case.
- $W \sim h$; i.e., the intermediate case in which h and W equal to within an order of magnitude or so.

Wide case. If $W \gg h$, most of the energy associated with propagating waves lies directly underneath the trace, and Figure 7.5 provides a relatively accurate impression of the fields in this region. The characteristic impedance Z_0 may be determined using the "lumped element" transmission line model using the following expression:

$$Z_0 = \sqrt{\frac{R' + j\omega L'}{G' + j\omega C'}} \tag{7.9}$$

where R', G', C', and L' are the resistance, conductance, capacitance, and inductance per unit length, respectively. For the present analysis, nothing is lost by assuming loss is negligible; therefore, let us assume $R' \ll \omega L'$ and $G' \ll \omega G'$, yielding

$$Z_0 \approx \sqrt{\frac{L'}{C'}} \tag{7.10}$$

Thus the problem is reduced to determining capacitance and inductance of the transmission line.

Wide microstrip line resembles a parallel-plate capacitor whose plate spacing d is very small compared to the plate area A. In this case, fringing fields may be considered negligible and one finds that the capacitance C is given by

$$C \approx \frac{\epsilon A}{d} \quad \text{(parallel plate capacitor)} \tag{7.11}$$

In terms of wide microstrip line, $A = Wl$ where l is length, and $d = h$. Therefore:

$$C' \triangleq \frac{C}{l} \approx \frac{\epsilon W}{h} \quad (W \gg h) \tag{7.12}$$

To determine L', consider the view of the microstrip line shown in Figure 7.6.

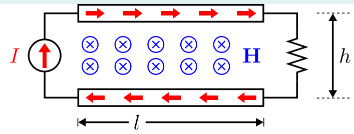

Figure 7.6. *View from the side of a microstrip line, used to determine L'.*

Here a current source applies a steady current I on the left, and a resistive load closes the current loop on the right. Ampere's law for magnetostatics and the associated "right hand rule" require that $\mathbf{H}$ is directed into the page and is approximately uniform. The magnetic flux between the trace and the ground plane is

$$\Phi = \int_{\mathcal{S}} \mathbf{B} \cdot d\mathbf{s} \tag{7.13}$$

where $\mathcal{S}$ is the surface bounded by the current loop and $\mathbf{B} = \mu_0 \mathbf{H}$. In the present problem, the area of $\mathcal{S}$ is hl and $\mathbf{H}$ is approximately constant over $\mathcal{S}$, so:

$$\Phi \approx \mu_0 H h l \tag{7.14}$$

where H is the magnitude of $\mathbf{H}$. Next, recall that:

$$L \triangleq \frac{\Phi}{I} \tag{7.15}$$

So, we may determine L if we are able to obtain an expression for I in terms of H. This can be done as follows. First, note that we can express I in terms of the current density on the trace; i.e.,

$$I = J_s W \tag{7.16}$$

where J_s is the current density (SI base units of A/m) on the trace. Next, we note that the boundary condition for $\mathbf{H}$ on the trace requires that the discontinuity in the tangent component of $\mathbf{H}$ going from the trace (where the magnetic field intensity is H) to beyond the trace (i.e., outside the transmission line, where the magnetic field intensity is approximately zero) be equal to the surface current. Thus, $J_s \approx H$ and

$$I = J_s W \approx H W \tag{7.17}$$

Returning to Equation 7.15, we find:

$$L \triangleq \frac{\Phi}{I} \approx \frac{\mu_0 H h l}{H W} = \frac{\mu_0 h l}{W} \tag{7.18}$$

Subsequently,

$$L' \triangleq \frac{L}{l} \approx \frac{\mu_0 h}{W} \quad (W \gg h) \tag{7.19}$$

Now the characteristic impedance is found to be

$$Z_0 \approx \sqrt{\frac{L'}{C'}} \approx \sqrt{\frac{\mu_0 h/W}{\epsilon W/h}} = \sqrt{\frac{\mu_0}{\epsilon}} \frac{h}{W} \tag{7.20}$$

The factor $\sqrt{\mu_0/\epsilon}$ is recognized as the wave impedance η. It is convenient to express this in terms of the free space wave impedance $\eta_0 \triangleq \sqrt{\mu_0/\epsilon_0}$, leading to the expression we seek:

$$\boxed{Z_0 \approx \frac{\eta_0}{\sqrt{\epsilon_r}} \frac{h}{W} \quad (W \gg h)} \tag{7.21}$$

The characteristic impedance of "wide" ($W \gg h$) microstrip line is given approximately by Equation 7.21.

It is worth noting that the characteristic impedance of wide transmission line is proportional to h/W. The factor h/W figures prominently in the narrow- and intermediate-width cases as well, as we shall soon see.

Narrow case. Figure 7.5 does not accurately depict the fields in the case that $W \ll h$. Instead, much of the energy associated with the electric and magnetic fields lies beyond and above the trace. Although these fields are relatively complex, we can develop a rudimentary model of the field structure by considering the relevant boundary conditions. In particular, the tangential component of $\mathbf{E}$ must be zero on the surfaces of the trace and ground plane. Also, we expect magnetic field lines to be perpendicular to the electric field lines so that the direction of propagation is along the axis of the line. These insights lead to Figure 7.7.

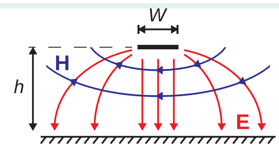

Figure 7.7. *Electric and magnetic fields lines for narrow ($W \ll h$) microstrip line.*

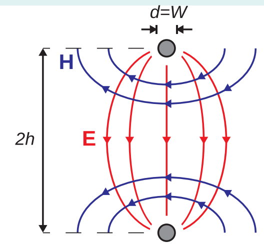

Figure 7.8. *Noting the similarity of the fields in narrow microstrip line to those in a parallel wire line.*

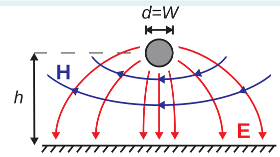

***Figure 7.9.** Modeling the fields in narrow microstrip line as those of a parallel wire line, now introducing the ground plane.*

Note that the field lines shown in Figure 7.7 are quite similar to those for parallel wire line (Section 7.1). If we choose diameter $d = W$ and wire spacing $D = 2h$, then the fields of the microstrip line in the dielectric spacer must be similar to those of the parallel wire line between the lines. This is shown in Figure 7.8. Note that the fields above the dielectric spacer in the microstrip line will typically be somewhat different (since the material above the trace is typically different; e.g., air). However, it remains true that we expect most of the energy to be contained in the dielectric, so we shall assume that this difference has a relatively small effect.

Next, we continue to refine the model by introducing the ground plane, as shown in Figure 7.9: The fields in the upper half-space are not perturbed when we do this, since the fields in Figure 7.8 already satisfy the boundary conditions imposed by the new ground plane. Thus, we see that the parallel wire transmission line provides a pretty good guide to the structure of the fields for the narrow transmission line, at least in the dielectric region of the upper half-space.

We are now ready to estimate the characteristic impedance $Z_0 \approx \sqrt{L'/C'}$ of low-loss narrow microstrip line. Neglecting the differences noted above, we estimate that this is roughly equal to the characteristic impedance of the analogous ($d = W$ and $D = 2h$) parallel wire line. Under this assumption, we obtain from Equation 7.8:

$$\boxed{Z_0 \sim \frac{1}{\pi}\frac{\eta_0}{\sqrt{\epsilon_r}}\ln\left(4h/W\right) \quad (W \ll h)} \tag{7.22}$$

This estimate will exhibit only "order of magnitude" accuracy (hence the "$\sim$" symbol), since the contribution from the fields in half of the relevant space is ignored. However we expect that Equation 7.22 will accurately capture the dependence of Z_0 on the parameters ϵ_r and h/W. These properties can be useful for making fine adjustments to a microstrip design.

The characteristic impedance of "narrow" ($W \ll h$) microstrip line can be roughly approximated by Equation 7.22.

Intermediate case. An expression for Z_0 in the intermediate case – even a rough estimate – is difficult to derive, and beyond the scope of this book. However, we are not completely in the dark, since we can reasonably anticipate that Z_0 in the intermediate case should be intermediate to estimates provided by the wide and narrow cases. This is best demonstrated by example. Figure 7.10 shows estimates of Z_0 using the wide and narrow expressions (blue and green curves, respectively) for a particular implementation of microstrip line (see Example 7.2 for details).

***Figure 7.10.** Z_0 for FR4 as a function of h/W, as determined by the "wide" and "narrow" approximations, along with the Wheeler 1977 formula. Note that the vertical and horizontal axes of this plot are in log scale.*

Since Z_0 varies smoothly with h/W, it is reasonable to expect that simply averaging the values generated using the wide and narrow assumptions would give a pretty good estimate when $h/W \sim 1$.

However, it is also possible to obtain an accurate estimate directly. A widely-accepted and broadly-applicable formula is provided in Wheeler 1977 (cited in “Additional Reading” at the end of this section). This expression is valid over the full range of h/W, not merely the intermediate case of $h/W \sim 1$. Here it is:

$$Z_0 \approx \frac{42.4\ \Omega}{\sqrt{\epsilon_r+1}} \times \ln\left[1+\frac{4h}{W'}\left(K+\sqrt{K^2+\frac{1+1/\epsilon_r}{2}\pi^2}\right)\right] \tag{7.23}$$

where

$$K \triangleq \frac{14+8/\epsilon_r}{11}\left(\frac{4h}{W'}\right) \tag{7.24}$$

and W' is W adjusted to account for the thickness t of the microstrip line. Typically $t \ll W$ and $t \ll h$, for which $W' \approx W$. Although complicated, this formula should not be completely surprising. For example, note the parameters h and W appear in this formula as the factor $4h/W$, which we encountered in the “narrow” approximation. Also, we see that the formula indicates Z_0 increases with increasing h/W and decreasing ϵ_r, as we determined in both the “narrow” and “wide” cases.

The following example provides a demonstration for the very common case of microstrip implementation in FR4 circuit board material.

Example

Example 7.2

Characteristic impedance of microstrip lines in FR4.

FR4 printed circuit boards consist of a substrate having $h \cong 1.575$ mm and $\epsilon_r \approx 4.5$. Figure 7.10 shows Z_0 as a function of h/W, as determined by the wide and narrow approximations, along with the value obtained using the Wheeler 1977 formula. The left side of the plot represents the wide condition, whereas the right side of this plot represents the narrow condition. The Wheeler 1977 formula is an accurate estimate over the entire horizontal span. Note that the wide approximation is accurate only for $h/W < 0.1$ or so, improving with decreasing h/W as expected. The narrow approximation overestimates Z_0 by a factor of about 1.4 (i.e., about 40%). This is consistent with our previous observation that this approximation should yield only about “order of magnitude” accuracy. Nevertheless, the narrow approximation exhibits approximately the same rate of increase with h/W as does the Wheeler 1977 formula.

Also worth noting from Figure 7.10 is the important and commonly-used result that $Z_0 \approx 50\ \Omega$ is obtained for $h/W \approx 0.5$. Thus, a $50\ \Omega$ microstrip line in FR4 has a trace width of about 3 mm.

A useful “take away” from this example is that the wide and narrow approximations serve as useful guides for understanding how Z_0 changes as a function of h/W and ϵ_r. This is useful especially for making adjustments to a microstrip line design once an accurate value of Z_0 is obtained from some other method; e.g., using the Wheeler 1977 formula or from measurements.

FR4 circuit board construction is so common that the result from the previous example deserves to be highlighted:

In FR4 printed circuit board construction (substrate thickness 1.575 mm, relative permittivity ≈ 4.5, negligible trace thickness), $Z_0 \approx 50\ \Omega$ requires a trace width of about 3 mm. Z_0 scales roughly in proportion to h/W around this value.

Simpler approximations for Z_0 are also commonly employed in the design and analysis of microstrip lines. These expressions are limited in the range of h/W for which they are valid, and can usually be shown to be special cases or approximations of Equation 7.23. Nevertheless, they are sometimes useful for quick “back of the envelope” calculations.

Wavelength in microstrip line. An accurate general formula for wavelength λ in microstrip line is similarly difficult to derive. A useful approximate technique employs a result from the theory of uniform plane waves in unbounded media. For such waves, the phase propagation constant β is given by

$$\beta = \omega\sqrt{\mu\epsilon} \tag{7.25}$$

It turns out that the electromagnetic field structure for the guided wave in a microstrip line is similar in the sense that it exhibits TEM field structure, as does the uniform plane wave. However, the guided wave is different in that it exists in both the dielectric spacer and the air above the spacer. Thus, we presume that β for the guided wave can be approximated as that of a uniform plane wave in unbounded media having the same permeability μ_0 but a different relative permittivity, which we shall assign the symbol $\epsilon_{r,eff}$ (for “*effective* relative permittivity”). Then:

$$\begin{aligned}\beta &\approx \omega\sqrt{\mu_0\ \epsilon_{r,eff}\ \epsilon_0} \quad \text{(low-loss microstrip)}\\ &= \beta_0\sqrt{\epsilon_{r,eff}}\end{aligned} \tag{7.26}$$

In other words, the phase propagation constant in a microstrip line can be approximated as the free-space phase propagation $\beta_0 \triangleq \omega\sqrt{\mu_0\epsilon_0}$ times a correction factor $\sqrt{\epsilon_{r,eff}}$.

Next, $\epsilon_{r,eff}$ is crudely approximated as the average of the relative permittivity of the dielectric slab and the relative permittivity of free space; i.e.,:

$$\epsilon_{r,eff} \approx \frac{\epsilon_r + 1}{2} \tag{7.27}$$

Various refinements exist to improve on this approximation; however, in practice, variations in the value of ϵ_r for the dielectric due to manufacturing processes typically make a more precise estimate irrelevant.

Using this concept, we obtain

$$\lambda = \frac{2\pi}{\beta} = \frac{2\pi}{\beta_0\sqrt{\epsilon_{r,eff}}} = \frac{\lambda_0}{\sqrt{\epsilon_{r,eff}}} \tag{7.28}$$

where λ_0 is the free-space wavelength c/f. Similarly the phase velocity v_p can be estimated using the relationship

$$v_p = \frac{\omega}{\beta} = \frac{c}{\sqrt{\epsilon_{r,eff}}} \tag{7.29}$$

i.e., the phase velocity in microstrip is slower than c by a factor of $\sqrt{\epsilon_{r,eff}}$.

Example

Example 7.3

Wavelength and phase velocity in microstrip in FR4 printed circuit boards.

FR4 is a low-loss fiberglass epoxy dielectric that is commonly used to make printed circuit boards (see "Additional Reading" at the end of this section). For FR4, $\epsilon_r \approx 4.5$. The effective relative permittivity is therefore:

$$\epsilon_{r,eff} \approx (4.5+1)/2 = 2.75$$

Thus, we estimate the phase velocity for the wave guided by this line to be about $c/\sqrt{2.75}$; i.e., 60% of c. Similarly, the wavelength of this wave is about 60% of the free space wavelength. In practice, these values are found to be slightly less; typically 50%–55%. The difference is attributable to the crude approximation of Equation 7.27.

Additional Reading:

- "Microstrip (https://en.wikipedia.org/wiki/Microstrip)" on Wikipedia.
- "Printed circuit board (https://en.wikipedia.org/wiki/Printed_circuit_board)" on Wikipedia.
- "Stripline (https://en.wikipedia.org/wiki/Stripline)" on Wikipedia.
- "Single-ended signaling (https://en.wikipedia.org/wiki/Single-ended_signaling)" on Wikipedia.
- Sec. 8.7 ("Differential Circuits") in S.W. Ellingson, *Radio Systems Engineering*, Cambridge Univ. Press, 2016.
- H.A. Wheeler, "Transmission Line Properties of a Strip on a Dielectric Sheet on a Plane," *IEEE Trans. Microwave Theory & Techniques*, Vol. 25, No. 8, Aug 1977, pp. 631–47.
- "FR-4 (https://en.wikipedia.org/wiki/FR-4)" on Wikipedia.

---

1. The reference in "Additional Reading" at the end of this section may be helpful if you are not familiar with this concept. ↩

7.3 Attenuation in Coaxial Cable

In this section, we consider the issue of attenuation in coaxial transmission line. Recall that attenuation can be interpreted in the context of the "lumped element" equivalent circuit transmission line model as the contributions of the resistance per unit length R' and conductance per unit length G'. In this model, R' represents the physical resistance in the inner and outer conductors, whereas G' represents loss due to current flowing directly between the conductors through the spacer material.

The parameters used to describe the relevant features of coaxial cable are shown in Figure 7.11. In this figure, a and b are the radii of the inner and outer conductors, respectively. σ_{ic} and σ_{oc} are the conductivities (SI base units of S/m) of the inner and outer conductors, respectively. Conductors are assumed to be non-magnetic; i.e., having permeability μ equal to the free space value μ_0. The spacer material is assumed to be a lossy dielectric having relative permittivity ϵ_r and conductivity σ_s.

Figure 7.11. *Parameters defining the design of a coaxial cable.*

Resistance per unit length. The resistance per unit length is the sum of the resistances of the inner and outer conductor per unit length. The resistance per unit length of the inner conductor is determined by σ_{ic} and the effective cross-sectional area through which the current flows. The latter is equal to the circumference $2\pi a$ times the skin depth δ_{ic} of the inner conductor, so:

$$R'_{ic} \approx \frac{1}{(2\pi a \cdot \delta_{ic})\,\sigma_{ic}} \quad \text{for } \delta_{ic} \ll a \tag{7.30}$$

This expression is only valid for $\delta_{ic} \ll a$ because otherwise the cross-sectional area through which the current flows is not well-modeled as a thin ring near the surface of the conductor. Similarly, we find the resistance per unit length of the outer conductor is

$$R'_{oc} \approx \frac{1}{(2\pi b \cdot \delta_{oc})\,\sigma_{oc}} \quad \text{for } \delta_{oc} \ll t \tag{7.31}$$

where δ_{oc} is the skin depth of the outer conductor and t is the thickness of the outer conductor. Therefore, the total resistance per unit length is

$$\begin{aligned} R' &= R'_{ic} + R'_{oc} \\ &\approx \frac{1}{(2\pi a \cdot \delta_{ic})\,\sigma_{ic}} + \frac{1}{(2\pi b \cdot \delta_{oc})\,\sigma_{oc}} \end{aligned} \tag{7.32}$$

Recall that skin depth depends on conductivity. Specifically:

$$\delta_{ic} = \sqrt{2/\omega\mu\sigma_{ic}} \tag{7.33}$$

$$\delta_{oc} = \sqrt{2/\omega\mu\sigma_{oc}} \tag{7.34}$$

Expanding Equation 7.32 to show explicitly the dependence on conductivity, we find:

$$R' \approx \frac{1}{2\pi\sqrt{2/\omega\mu_0}}\left[\frac{1}{a\sqrt{\sigma_{ic}}} + \frac{1}{b\sqrt{\sigma_{oc}}}\right] \tag{7.35}$$

At this point it is convenient to identify two particular cases for the design of the cable. In the first case, “Case I,” we assume $\sigma_{oc} \gg \sigma_{ic}$. Since $b > a$, we have in this case

$$\begin{aligned} R' &\approx \frac{1}{2\pi\sqrt{2/\omega\mu_0}} \left[\frac{1}{a\sqrt{\sigma_{ic}}}\right] \\ &= \frac{1}{2\pi\delta_{ic}\sigma_{ic}} \; \frac{1}{a} \quad \text{(Case I)} \end{aligned} \tag{7.36}$$

In the second case, “Case II,” we assume $\sigma_{oc} = \sigma_{ic}$. In this case, we have

$$\begin{aligned} R' &\approx \frac{1}{2\pi\sqrt{2/\omega\mu_0}} \left[\frac{1}{a\sqrt{\sigma_{ic}}} + \frac{1}{b\sqrt{\sigma_{ic}}}\right] \\ &= \frac{1}{2\pi\delta_{ic}\sigma_{ic}} \; \left[\frac{1}{a} + \frac{1}{b}\right] \quad \text{(Case II)} \end{aligned} \tag{7.37}$$

A simpler way to deal with these two cases is to represent them both using the single expression

$$R' \approx \frac{1}{2\pi\delta_{ic}\sigma_{ic}} \; \left[\frac{1}{a} + \frac{C}{b}\right] \tag{7.38}$$

where $C = 0$ in Case I and $C = 1$ in Case II.

Conductance per unit length. The conductance per unit length of coaxial cable is simply that of the associated coaxial structure at DC; i.e.,

$$G' = \frac{2\pi\sigma_s}{\ln(b/a)} \tag{7.39}$$

Unlike resistance, the conductance is independent of frequency, at least to the extent that σ_s is independent of frequency.

Attenuation. The attenuation of voltage and current waves as they propagate along the cable is represented by the factor $e^{-\alpha z}$, where z is distance traversed along the cable. It is possible to find an expression for α in terms of the material and geometry parameters using:

$$\gamma \triangleq \sqrt{(R' + j\omega L')(G' + j\omega C')} = \alpha + j\beta \tag{7.40}$$

where L' and C' are the inductance per unit length and capacitance per unit length, respectively. These are given by

$$L' = \frac{\mu}{2\pi}\ln(b/a) \tag{7.41}$$

and

$$C' = \frac{2\pi\epsilon_0\epsilon_r}{\ln(b/a)} \tag{7.42}$$

In principle we could solve Equation 7.40 for α. However, this course of action is quite tedious, and a simpler approximate approach facilitates some additional insights. In this approach, we define parameters α_R associated with R' and α_G associated with G' such that

$$e^{-\alpha_R z} e^{-\alpha_G z} = e^{-(\alpha_R + \alpha_G) z} = e^{-\alpha z} \tag{7.43}$$

which indicates

$$\alpha = \alpha_R + \alpha_G \tag{7.44}$$

Next we postulate

$$\alpha_R \approx K_R \frac{R'}{Z_0} \tag{7.45}$$

where Z_0 is the characteristic impedance

$$Z_0 \approx \frac{\eta_0}{2\pi} \frac{1}{\sqrt{\epsilon_r}} \ln \frac{b}{a} \quad \text{(low loss)} \tag{7.46}$$

and where K_R is a unitless constant to be determined. The justification for Equation 7.45 is as follows: First, α_R must increase monotonically with increasing R'. Second, R' must be divided by an impedance in order to obtain the correct units of 1/m. Using similar reasoning, we postulate

$$\alpha_G \approx K_G G' Z_0 \tag{7.47}$$

where K_G is a unitless constant to be determined. The following example demonstrates the validity of Equations 7.45 and 7.47, and will reveal the values of K_R and K_G.

Example

Example 7.4

Attenuation constant for RG-59.

RG-59 is a popular form of coaxial cable having the parameters $a \cong 0.292$ mm, $b \cong 1.855$ mm, $\sigma_{ic} \cong 2.28 \times 10^7$ S/m, $\sigma_s \cong 5.9 \times 10^{-5}$ S/m, and $\epsilon_r \cong 2.25$. The conductivity σ_{oc} of the outer conductor is difficult to quantify because it consists of a braid of thin metal strands. However, $\sigma_{oc} \gg \sigma_{ic}$, so we may assume Case I; i.e., $\sigma_{oc} \gg \sigma_{ic}$, and subsequently $C = 0$. Figure 7.12 shows the components α_G and α_R computed for the particular choice $K_R = K_G = 1/2$. The figure also shows $\alpha_G + \alpha_R$, along with α computed using Equation 7.40. We find that the agreement between these values is very good, which is compelling evidence that the ansatz is valid and $K_R = K_G = 1/2$.

Figure 7.12. *Comparison of $\alpha = \mathrm{Re}\{\gamma\}$ to α_R, α_G, and $\alpha_R + \alpha_G$ for $K_R = K_G = 1/2$. The result for α has been multiplied by 1.01; otherwise the curves would be too close to tell apart.*

Note that there is nothing to indicate that the results demonstrated in the example are not generally true. Thus, we come to the following conclusion:

The attenuation constant $\alpha \approx \alpha_G + \alpha_R$ where $\alpha_G \triangleq R'/2Z_0$ and $\alpha_R \triangleq G'Z_0/2$.

Minimizing attenuation. Let us now consider if there are design choices which minimize the attenuation of coaxial cable. Since $\alpha = \alpha_R + \alpha_G$, we may consider α_R and α_G independently. Let us first consider α_G:

$$\begin{aligned} \alpha_G &\triangleq \frac{1}{2} G' Z_0 \\ &\approx \frac{1}{2} \cdot \frac{2\pi\sigma_s}{\ln(b/a)} \cdot \frac{1}{2\pi} \frac{\eta_0}{\sqrt{\epsilon_r}} \ln(b/a) \\ &= \frac{\eta_0}{2} \frac{\sigma_s}{\sqrt{\epsilon_r}} \end{aligned} \tag{7.48}$$

It is clear from this result that α_G is minimized by minimizing $\sigma_s/\sqrt{\epsilon_r}$. Interestingly the physical dimensions a and b have no discernible effect on α_G.

Now we consider α_R:

$$\begin{aligned} \alpha_R &\triangleq \frac{R'}{2Z_0} \\ &= \frac{1}{2} \frac{(1/2\pi\delta_{ic}\sigma_{ic})\,[1/a + C/b]}{(1/2\pi)\,(\eta_0/\sqrt{\epsilon_r})\ln(b/a)} \\ &= \frac{\sqrt{\epsilon_r}}{2\eta_0\delta_{ic}\sigma_{ic}} \cdot \frac{[1/a + C/b]}{\ln(b/a)} \end{aligned} \tag{7.49}$$

Now making the substitution $\delta_{ic} = \sqrt{2/\omega\mu_0\sigma_{ic}}$ in order to make the dependences on the constitutive parameters explicit, we find:

$$\alpha_R = \frac{1}{2\sqrt{2}\cdot\eta_0}\sqrt{\frac{\omega\mu_0\epsilon_r}{\sigma_{ic}}}\cdot\frac{[1/a + C/b]}{\ln(b/a)} \tag{7.50}$$

Here we see that α_R is minimized by minimizing ϵ_r/σ_{ic}. It's not surprising to see that we should maximize σ_{ic}. However, it's a little surprising that we should minimize ϵ_r. Furthermore, this is in contrast to α_G, which is minimized by *maximizing* ϵ_r. Clearly there is a tradeoff to be made here. To determine the parameters of this tradeoff, first note that the result depends on frequency: Since α_R dominates over α_G at sufficiently high frequency (as demonstrated in Figure 7.12), it seems we should minimize ϵ_r if the intended frequency of operation is sufficiently high; otherwise the optimum value is frequency-dependent. However, σ_s may vary as a function of ϵ_r, so a general conclusion about optimum values of σ_s and ϵ_r is not appropriate.

However, we also see that α_R – unlike α_G – depends on a and b. This implies the existence of a generally-optimum geometry. To find this geometry, we minimize α_R by taking the derivative with respect to a, setting the result equal to zero, and solving for a and/or b. Here we go:

$$\frac{\partial}{\partial a}\alpha_R = \frac{1}{2\sqrt{2}\cdot\eta_0}\sqrt{\frac{\omega\mu_0\epsilon_r}{\sigma_{ic}}}\cdot\frac{\partial}{\partial a}\frac{[1/a + C/b]}{\ln(b/a)} \tag{7.51}$$

This derivative is worked out in an addendum at the end of this section. Using the result from the addendum, the right side of Equation 7.51 can be written as follows:

$$\frac{1}{2\sqrt{2}\cdot\eta_0}\sqrt{\frac{\omega\mu_0\epsilon_r}{\sigma_{ic}}}\cdot\left[\frac{-1}{a^2\ln(b/a)} + \frac{1/a + C/b}{a\ln^2(b/a)}\right] \tag{7.52}$$

In order for $\partial\alpha_R/\partial a = 0$, the factor in the square brackets above must be equal to zero. After a few steps of algebra, we find:

$$\ln(b/a) = 1 + \frac{C}{b/a} \tag{7.53}$$

In Case I ($\sigma_{oc} \gg \sigma_{ic}$), $C = 0$ so:

$$b/a = e \cong 2.72 \quad \text{(Case I)} \tag{7.54}$$

In Case II ($\sigma_{oc} = \sigma_{ic}$), $C = 1$. The resulting equation can be solved by plotting the function, or by a few iterations of trial and error; either way one quickly finds

$$b/a \cong 3.59 \quad \text{(Case II)} \tag{7.55}$$

Summarizing, we have found that α is minimized by choosing the ratio of the outer and inner radii to be somewhere between 2.72 and 3.59, with the precise value depending on the relative conductivity of the inner and outer conductors.

Substituting these values of b/a into Equation 7.46, we obtain:

$$Z_0 \approx \frac{59.9\ \Omega}{\sqrt{\epsilon_r}} \ \text{ to } \ \frac{76.6\ \Omega}{\sqrt{\epsilon_r}} \tag{7.56}$$

as the range of impedances of coaxial cable corresponding to physical designs that minimize attenuation.

Equation 7.56 gives the range of characteristic impedances that minimize attenuation for coaxial transmission lines. The precise value within this range depends on the ratio of the conductivity of the outer conductor to that of the inner conductor.

Since $\epsilon_r \geq 1$, the impedance that minimizes attenuation is less for dielectric-filled cables than it is for air-filled cables. For example, let us once again consider the RG-59 from Example 7.4. In that case, $\epsilon_r \cong 2.25$ and $C = 0$, indicating Z_0 $\approx 39.9\ \Omega$ is optimum for attenuation. The actual characteristic impedance of Z_0 is about $75\ \Omega$, so clearly RG-59 is not optimized for attenuation. This is simply because other considerations apply, including power handling capability (addressed in Section 7.4) and the convenience of standard values (addressed in Section 7.5).

Addendum: Derivative of $a^2 \ln(b/a)$. Evaluation of Equation 7.51 requires finding the derivative of $a^2 \ln(b/a)$ with respect to a. Using the chain rule, we find:

$$\begin{aligned} \frac{\partial}{\partial a}\left[a^2 \ln\left(\frac{b}{a}\right)\right] = &\left[\frac{\partial}{\partial a}a^2\right]\ln\left(\frac{b}{a}\right) \\ &+a^2\left[\frac{\partial}{\partial a}\ln\left(\frac{b}{a}\right)\right] \end{aligned} \tag{7.57}$$

Note

$$\frac{\partial}{\partial a}a^2 = 2a \tag{7.58}$$

and

$$\begin{aligned} \frac{\partial}{\partial a}\ln\left(\frac{b}{a}\right) &= \frac{\partial}{\partial a}\left[\ln\left(b\right) - \ln\left(a\right)\right] \\ &= -\frac{\partial}{\partial a}\ln\left(a\right) \\ &= -\frac{1}{a} \end{aligned} \tag{7.59}$$

So:

$$\begin{aligned} \frac{\partial}{\partial a}\left[a^2 \ln\left(\frac{b}{a}\right)\right] &= \left[2a\right]\ln\left(\frac{b}{a}\right) + a^2\left[-\frac{1}{a}\right] \\ &= \boxed{2a\ln\left(\frac{b}{a}\right) - a} \end{aligned} \tag{7.60}$$

This result is substituted for $a^2 \ln(b/a)$ in Equation 7.51 to obtain Equation 7.52.

7.4 Power Handling Capability of Coaxial Cable

The term “power handling” refers to maximum power that can be safely transferred by a transmission line. This power is limited because when the electric field becomes too large, dielectric breakdown and arcing may occur. This may result in damage to the line and connected devices, and so must be avoided. Let E_{pk} be the maximum safe value of the electric field intensity within the line, and let P_{max} be the power that is being transferred under this condition. This section addresses the following question: How does one design a coaxial cable to maximize P_{max} for a given E_{pk}?

We begin by finding the electric potential V within the cable. This can be done using Laplace’s equation:

$$\nabla^2 V = 0 \tag{7.61}$$

Using the cylindrical (ρ, ϕ, z) coordinate system with the z axis along the inner conductor, we have $\partial V/\partial\phi = 0$ due to symmetry. Also we set $\partial V/\partial z = 0$ since the result should not depend on z. Thus, we have:

$$\frac{1}{\rho}\frac{\partial}{\partial\rho}\left(\rho\frac{\partial V}{\partial\rho}\right) = 0 \tag{7.62}$$

Solving for V, we have

$$V(\rho) = A\ln\rho + B \tag{7.63}$$

where A and B are arbitrary constants, presumably determined by boundary conditions. Let us assume a voltage V_0 measured from the inner conductor (serving as the “$+$” terminal) to the outer conductor (serving as the “$-$” terminal). For this choice, we have:

$$V(a) = V_0 \quad \rightarrow \quad A\ln a + B = V_0 \tag{7.64}$$
$$V(b) = 0 \quad \rightarrow \quad A\ln b + B = 0 \tag{7.65}$$

Subtracting the second equation from the first and solving for A, we find $A = -V_0/\ln(b/a)$. Subsequently, B is found to be $V_0\ln(b)/\ln(b/a)$, and so

$$V(\rho) = \frac{-V_0}{\ln(b/a)}\ln\rho + \frac{V_0\ln(b)}{\ln(b/a)} \tag{7.66}$$

The electric field intensity is given by:

$$\mathbf{E} = -\nabla V \tag{7.67}$$

Again we have $\partial V/\partial\phi = \partial V/\partial z = 0$, so

$$\mathbf{E} = -\hat{\rho}\frac{\partial}{\partial\rho}V \tag{7.68}$$
$$= -\hat{\rho}\frac{\partial}{\partial\rho}\left[\frac{-V_0}{\ln(b/a)}\ln\rho + \frac{V_0\ln(b)}{\ln(b/a)}\right] \tag{7.69}$$
$$= +\hat{\rho}\frac{V_0}{\rho\ln(b/a)} \tag{7.70}$$

Note that the maximum electric field intensity in the spacer occurs at $\rho = a$; i.e., at the surface of the inner conductor. Therefore:

$$E_{pk} = \frac{V_0}{a \ln(b/a)} \tag{7.71}$$

The power transferred by the line is maximized when the impedances of the source and load are matched to Z_0. In this case, the power transferred is $V_0^2/2Z_0$. Recall that the characteristic impedance Z_0 is given in the “low-loss” case as

$$Z_0 \approx \frac{1}{2\pi}\frac{\eta_0}{\sqrt{\epsilon_r}}\ln\left(\frac{b}{a}\right) \tag{7.72}$$

Therefore, the maximum safe power is

$$\begin{align} P_{max} &= \frac{V_0^2}{2Z_0} \tag{7.73}\\ &\approx \frac{E_{pk}^2\ a^2 \ln^2(b/a)}{2\cdot(1/2\pi)\left(\eta_0/\sqrt{\epsilon_r}\right)\ln(b/a)} \tag{7.74}\\ &= \frac{\pi E_{pk}^2}{\eta_0/\sqrt{\epsilon_r}}\ a^2 \ln(b/a) \tag{7.75} \end{align}$$

Now let us consider if there is a value of a which maximizes P_{max}. We do this by seeing if $\partial P_{max}/\partial a = 0$ for some values of a and b. The derivative is worked out in an addendum at the end of this section. Using the result from the addendum, we find:

$$\frac{\partial}{\partial a}P_{max} = \frac{\pi E_{pk}^2}{\eta_0/\sqrt{\epsilon_r}}\ \left[2a\ln(b/a) - a\right] \tag{7.76}$$

For the above expression to be zero, it must be true that $2\ln(b/a) - 1 = 0$. Solving for b/a, we obtain:

$$\frac{b}{a} = \sqrt{e} \cong 1.65 \tag{7.77}$$

for optimum power handling. In other words, 1.65 is the ratio of the radii of the outer and inner conductors that maximizes the power that can be safely handled by the cable.

Equation 7.75 suggests that ϵ_r should be maximized in order to maximize power handling, and you wouldn’t be wrong for noting that, however, there are some other factors that may indicate otherwise. For example, a material with higher ϵ_r may also have higher σ_s, which means more current flowing through the spacer and thus more ohmic heating. This problem is so severe that cables that handle high RF power often use air as the spacer, even though it has the *lowest* possible value of ϵ_r. Also worth noting is that σ_{ic} and σ_{oc} do not matter according to the analysis we’ve just done; however, to the extent that limited conductivity results in significant ohmic heating in the conductors – which we have also not considered – there may be something to consider. Suffice it to say, the actionable finding here concerns the ratio of the radii; the other parameters have not been suitably constrained by this analysis.

Substituting $\sqrt{e}$ for b/a in Equation 7.72, we find:

$$Z_0 \approx \frac{30.0\ \Omega}{\sqrt{\epsilon_r}} \tag{7.78}$$

This is the characteristic impedance of coaxial line that optimizes power handling, subject to the caveats identified above. For air-filled cables, we obtain $30\ \Omega$. Since $\epsilon_r \geq 1$, this optimum impedance is less for dielectric-filled cables than it is for air-filled cables.

Summarizing:

> The power handling capability of coaxial transmission line is optimized when the ratio of radii of the outer to inner conductors b/a is about 1.65. For the air-filled cables typically used in high-power applications, this corresponds to a characteristic impedance of about $30\ \Omega$.

Addendum: Derivative of $(1/a + C/b) / \ln(b/a)$. Evaluation of Equation 7.75 requires finding the derivative of $(1/a + C/b) / \ln(b/a)$ with respect to a. Using the chain rule, we find:

$$\begin{aligned}\frac{\partial}{\partial a}\left[\frac{1/a + C/b}{\ln(b/a)}\right] = &\left[\frac{\partial}{\partial a}\left(\frac{1}{a}+\frac{C}{b}\right)\right]\ln^{-1}\left(\frac{b}{a}\right) \\ &+ \left(\frac{1}{a}+\frac{C}{b}\right)\left[\frac{\partial}{\partial a}\ln^{-1}\left(\frac{b}{a}\right)\right]\end{aligned} \tag{7.79}$$

Note

$$\frac{\partial}{\partial a}\left(\frac{1}{a}+\frac{C}{b}\right) = -\frac{1}{a^2} \tag{7.80}$$

To handle the quantity in the second set of square brackets, first define $v = \ln u$, where $u = b/a$. Then:

$$\begin{aligned}\frac{\partial}{\partial a}v^{-1} &= \left[\frac{\partial}{\partial v}v^{-1}\right]\left[\frac{\partial v}{\partial u}\right]\left[\frac{\partial u}{\partial a}\right] \\ &= \left[-v^{-2}\right]\left[\frac{1}{u}\right]\left[-ba^{-2}\right] \\ &= \left[-\ln^{-2}\left(\frac{b}{a}\right)\right]\left[\frac{a}{b}\right]\left[-ba^{-2}\right] \\ &= \frac{1}{a}\ln^{-2}\left(\frac{b}{a}\right)\end{aligned} \tag{7.81}$$

So:

$$\begin{aligned}\frac{\partial}{\partial a}\left[\frac{1/a + C/b}{\ln(b/a)}\right] = &\left[-\frac{1}{a^2}\right]\ln^{-1}\left(\frac{b}{a}\right) \\ &+ \left(\frac{1}{a}+\frac{C}{b}\right)\left[\frac{1}{a}\ln^{-2}\left(\frac{b}{a}\right)\right]\end{aligned} \tag{7.82}$$

This result is substituted in Equation 7.75 to obtain Equation 7.76.

7.5 Why 50 Ohms?

The quantity $50\ \Omega$ appears in a broad range of applications across the field of electrical engineering. In particular, it is a very popular value for the characteristic impedance of transmission line, and is commonly specified as the port impedance for signal sources, amplifiers, filters, antennas, and other RF components. So, what's special about $50\ \Omega$? The short answer is "nothing." In fact, other standard impedances are in common use – prominent among these is $75\ \Omega$. It is shown in this section that a broad range of impedances – on the order of 10s of ohms – emerge as useful values based on technical considerations such as minimizing attenuation, maximizing power handling, and compatibility with common types of antennas. Characteristic impedances up to $300\ \Omega$ and beyond are useful in particular applications. However, it is not practical or efficient to manufacture and sell products for every possible impedance in this range. Instead, engineers have settled on $50\ \Omega$ as a round number that lies near the middle of this range, and have chosen a few other values to accommodate the smaller number of applications where there may be specific compelling considerations.

So, the question becomes "what makes characteristic impedances in the range of 10s of ohms particularly useful?" One consideration is attenuation in coaxial cable. Coaxial cable is by far the most popular type of transmission line for connecting devices on separate printed circuit boards or in separate enclosures. The attenuation of coaxial cable is addressed in Section 7.3. In that section, it is shown that attenuation is minimized for characteristic impedances in the range $(60\ \Omega)/\sqrt{\epsilon_r}$ to $(77\ \Omega)/\sqrt{\epsilon_r}$, where ϵ_r is the relative permittivity of the spacer material. So, we find that Z_0 in the range $60\ \Omega$ to $77\ \Omega$ is optimum for air-filled cable, but more like $40\ \Omega$ to $50\ \Omega$ for cables using a plastic spacer material having typical $\epsilon_r \approx 2.25$. Thus, $50\ \Omega$ is clearly a reasonable choice if a single standard value is to be established for all such cable.

Coaxial cables are often required to carry high power signals. In such applications, power handling capability is also important, and is addressed in Section 7.4. In that section, we find the power handling capability of coaxial cable is optimized when the ratio of radii of the outer to inner conductors b/a is about 1.65. For the air-filled cables typically used in high-power applications, this corresponds to a characteristic impedance of about $30\ \Omega$. This is significantly less than the $60\ \Omega$ to $77\ \Omega$ that minimizes attenuation in air-filled cables. So, $50\ \Omega$ can be viewed as a compromise between minimizing attenuation and maximizing power handling in air-filled coaxial cables.

Although the preceding arguments justify $50\ \Omega$ as a standard value, one can also see how one might make a case for $75\ \Omega$ as a secondary standard value, especially for applications where attenuation is the primary consideration.

Values of $50\ \Omega$ and $75\ \Omega$ also offer some convenience when connecting RF devices to antennas. For example, $75\ \Omega$ is very close to the impedance of the commonly-encountered half-wave dipole antenna (about $73 + j42\ \Omega$), which may make impedance matching to that antenna easier. Another commonly-encountered antenna is the quarter-wave monopole, which exhibits an impedance of about $36 + j21\ \Omega$, which is close to $50\ \Omega$. In fact, we see that if we desire a single characteristic impedance that is equally convenient for applications involving either type of antenna, then $50\ \Omega$ is a reasonable choice.

A third commonly-encountered antenna is the *folded* half-wave dipole. This type of antenna is similar to a half-wave dipole but has better bandwidth, and is commonly used in FM and TV systems and land mobile radio (LMR) base stations. A folded half-wave dipole has an impedance of about $300\ \Omega$ and is balanced (not single-ended); thus, there is a market for balanced transmission line having $Z_0 = 300\ \Omega$. However, it is very easy and inexpensive to implement a balun (a device which converts the dipole output from balanced to unbalanced) while simultaneously stepping down impedance by a factor of 4; i.e., to $75\ \Omega$. Thus, we have an additional application for $75\ \Omega$ coaxial line.

Finally, note that it is quite simple to implement microstrip transmission line having characteristic impedance in the range $30\ \Omega$ to $75\ \Omega$. For example, $50\ \Omega$ on commonly-used 1.575 mm FR4 requires a width-to-height ratio of about 2, so the trace is about 3 mm wide. This is a very manageable size and easily implemented in printed circuit board designs.

Additional Reading:

- “Dipole antenna (https://en.wikipedia.org/wiki/Dipole_antenna)” on Wikipedia.
- “Monopole antenna (https://en.wikipedia.org/wiki/Monopole_antenna)” on Wikipedia.
- “Balun (https://en.wikipedia.org/wiki/Balun)” on Wikipedia.

End Matter

Image Credits

- **Fig.** 7.1: © SpinningSpark, Inductiveload, https://commons.wikimedia.org/wiki/File:Twin-lead_cable_dimension.svg (https://commons.wikimedia.org/wiki/File:Twin-lead_cable_dimension.svg), CC BY-SA 3.0 (https://creativecommons.org/licenses/by-sa/3.0/ (https://creativecommons.org/licenses/by-sa/3.0/)). Minor modifications.
- **Fig.** 7.2: © Sevenchw (C. Wang), https://commons.wikimedia.org/wiki/File:Parallel_wire_transmission_line_structure_and_design_parameters.svg (https://commons.wikimedia.org/wiki/File:Parallel_wire_transmission_line_structure_and_design_parameters.svg), CC BY-SA 4.0 (https://creativecommons.org/licenses/by-sa/4.0/ (https://creativecommons.org/licenses/by-sa/4.0/)).
- **Fig.** 7.3: © Offaperry (S. Lally), https://commons.wikimedia.org/wiki/File:Electric_and_Magnetic_Field_of_Wire_Cross-Section.svg (https://commons.wikimedia.org/wiki/File:Electric_and_Magnetic_Field_of_Wire_Cross-Section.svg), CC BY-SA 4.0 (https://creativecommons.org/licenses/by-sa/4.0/ (https://creativecommons.org/licenses/by-sa/4.0/)).
- **Fig.** 7.4: © 7head7metal7, https://commons.wikimedia.org/wiki/File:Microstrip_scheme.svg (https://commons.wikimedia.org/wiki/File:Microstrip_scheme.svg), CC BY-SA 3.0 (https://creativecommons.org/licenses/by-sa/3.0/ (https://creativecommons.org/licenses/by-sa/3.0/)). Minor modifications from the original.
- **Fig.** 7.6: © Sevenchw (C. Wang), https://commons.wikimedia.org/wiki/File:View_from_the_side_of_a_microstrip_line.svg (https://commons.wikimedia.org/wiki/File:View_from_the_side_of_a_microstrip_line.svg), CC BY-SA 4.0 (https://creativecommons.org/licenses/by-sa/4.0/ (https://creativecommons.org/licenses/by-sa/4.0/)).
- **Fig.** 7.7: © Offaperry (S. Lally), https://commons.wikimedia.org/wiki/File:Electric_and_Magnetic_Fields_for_Microstrip.svg (https://commons.wikimedia.org/wiki/File:Electric_and_Magnetic_Fields_for_Microstrip.svg), CC BY-SA 4.0 (https://creativecommons.org/licenses/by-sa/4.0/ (https://creativecommons.org/licenses/by-sa/4.0/)).